Isolated Grid-Forming Control of Wave Energy Converter for Island Electrification

Ullah, Md Imran; Hashfi, Tuanku Badzlin; Döhler, Jessica S.; De Albuquerque, Vinicius M.; Aitkulova, Aisuluu; Forslund, Johan; Boström, Cecilia; Wahyudie, Addy; Temiz, Irina

DOI
10.1109/ACCESS.2025.3552820

Publication date
2025

Document Version
Final published version

Published in
IEEE Access

IEEE Access
Multidisciplinary | Rapid Review | Open Access Journal

Received 23 February 2025, accepted 12 March 2025, date of publication 19 March 2025, date of current version 27 March 2025.

Digital Object Identifier 10.1109/ACCESS.2025.3552820

RESEARCH ARTICLE

Isolated Grid-Forming Control of Wave Energy Converter for Island Electrification

MD IMRAN ULLAH[1], (Graduate Student Member, IEEE), TUANKU BADZLIN HASHFI[2], (Graduate Student Member, IEEE), JESSICA S. DÖHLER[1], VINICIUS M. DE ALBUQUERQUE[1], AISULUU AITKULOVA[1], JOHAN FORSLUND[1], CECILIA BOSTRÖM[1], ADDY WAHYUDIE[3], AND IRINA TEMIZ[1]

[1]Department of Electrical Engineering, Uppsala University, 753 10 Uppsala, Sweden
[2]Electrical Sustainable Energy, Delft University of Technology, 2628 CD Delft, The Netherlands
[3]Department of Electrical Engineering, United Arab Emirates University, Al Ain, United Arab Emirates

Corresponding author: Md Imran Ullah (imran.ullah@angstrom.uu.se)

This work was supported in part by the Department of Electrical Engineering, Uppsala University, Sweden; in part by the Department of Electrical Engineering, United Arab Emirates University, Al Ain, United Arab Emirates; in part by the Sederholms Travel Abroad Grant; in part by STandUP for Energy, Sweden; and in part by the EU-SCORES Project by the European Union's Horizon 2020 and Green Deal Research and Innovation Programme under Grant 101036457.

ABSTRACT As the world transitions to renewable electrification to reduce CO_2 emissions, remote island electrification remains a challenge. Although some islands are connected to the grid, many still rely on fossil fuels for electricity generation. Several studies indicate that renewable energy sources, such as wave energy, have the potential to make these islands self-reliant because of their substantial power potential. However, research on the control of power electronics converters for these systems remains limited. This paper proposes isolated grid-forming control for island electrification to address this gap using a wave energy converter and an energy storage system. Resistive loading control is implemented to optimize the power absorption of the generator. The result illustrates the establishment of the required AC voltage and 50 Hz frequency in the island load, ensuring harmonics compliance with the recommended standards. Experiments were conducted to test and validate the operation of different converter controls. The results also demonstrate the converter's ability to black-start the island load and automatically transition the load current with varying loads in a few milliseconds. Furthermore, the power quality produced by the wave energy converter presents one of its significant challenges. Therefore, the performance of two distinct converter technologies was compared. The performance of the IGBT converter was evaluated against that of the SiC-based converter in terms of power quality. The study demonstrates that the use of SiC enhances power quality in all switching frequencies tested, achieving the most significant reduction of 78% in current THD and 92% in voltage THD at the 25 kHz switching frequency, thus validating its advantages for wave energy converter applications.

INDEX TERMS Wave energy, control system, island electrification, grid-forming, energy storage system control, power quality, harmonics mitigation.

I. INTRODUCTION

Electrifying an island has always posed significant challenges due to its financial and technical constraints [1], [2]. These constraints are mainly due to the vast distance from the mainland grid connection or the power generation. Connecting a distant island to the mainland grid involves substantial investment costs for the country's Transmission System Operator (TSO). While some islands are grid-connected [3], many rely on coal and diesel for energy [4]. An island's reliance on fossil fuels for electricity poses several threats at various levels [5]. These include carbon emissions, the risk of spillage during fuel transportation, and air and noise pollution from running diesel generators [6],

The associate editor coordinating the review of this manuscript and approving it for publication was Tao Wang.

[7], [8]. Additionally, the dependence on fossil fuels makes the island's electricity cost higher and vulnerable to fuel price fluctuations, which are influenced by geopolitical events and international relations [9], [10]. Due to these disadvantages, renewable energy or hybrid renewable energy systems with batteries can replace fossil fuels for stable electricity generation, making the island self-reliant and sustainable [11].

The integration of renewable energy systems presents several technical challenges, including the technology's early stage of development, unpredictability due to intermittency, and issues such as harmonics and flicker [12]. As a result, maintaining reliability, stability, and consistent power quality is a significant challenge [13]. In addition, investment costs, the complexities of managing variable energy systems, and potential environmental concerns, such as landscape degradation, particularly on islands, maintenance requirements, transportation, and logistics of deployment, can be considerable [2]. However, a research study has concluded that making an island self-sustained by using renewable energy can protect its local environment by reducing the cost of power generation while ensuring a stable power supply [14]. Several techno-economic and socio-economic studies for electrifying islands using renewable energy have also been done [15], [16], [17]. Ahmad and Zhang performed a techno-economic feasibility analysis of both grid connected and islanded operation of renewable energy integration on an island [15]. Whereas, Bertheau performed geospatial and techno-economic analysis for an island in the Philippines being supplied fully using renewable energy, estimating the supply cost [16]. Prieto et al. studied the socio-economic and environmental factors of employing wave energy in Gran Canaria Island, Spain [17]. Previous research has often used the island's natural resources data such as solar irradiation, wind speed or significant wave height and frequency to suggest different renewable energy technologies to optimize the energy required on the island. However, ensuring a stable, reliable power supply on the island, the design of electrical networks and their controls still remains a major challenge.

Renewable energies such as wave energy, wind energy, hydropower, and solar energy are common resources that can be used to generate electricity for island electrification [13], [18], [19], [20]. Kuang et al. investigated different renewable energy resources and technologies such as wind energy, solar energy, hydropower, biomass, ocean and geothermal energy for island electrification [13]. Few researches have noted that wave energy has a slight advantage over wind and solar energy due to its higher energy density [21], greater predictability [22], and more continuous power throughout the day [23]. Its seasonal variation also makes it well-suited to meet the electricity demand on a few islands where the energy demand is higher during the winter and milder during the summer [24], [25], [26]. Additionally, wave energy can also be a cost-effective solution for remote communities, such as islands, which is the focus of the current study. Building a small-scale hydropower plant in such areas

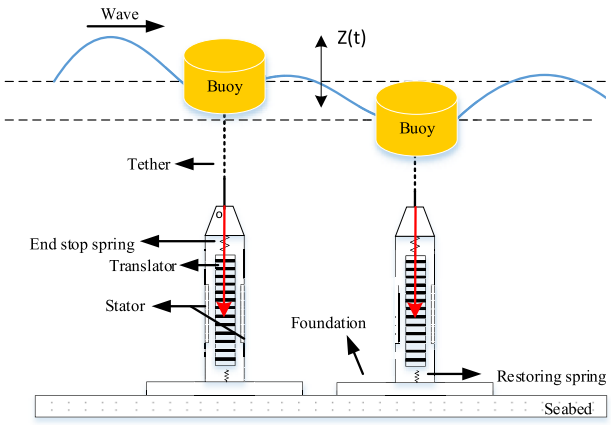

FIGURE 1. Wave energy converter.

can be cost-prohibitive due to the high capital expenses associated with design and permitting. A research study has demonstrated that in these scenarios, wave energy can offer economic benefits if the power is supplied at a cost below $0.59/kWh [18]. However, despite its power potential, several technical and operational challenges still remain in electrifying islands using renewable energy [2].

To address technical issues, implementing energy storage systems, advanced forecasting techniques, and controls can help balance supply and demand, ensuring a reliable and high-quality power supply. Additionally, it is also essential to reach local consensus, engage in dialogues, and communicate the economic impacts to the community when setting up renewable energy generation on islands [2]. Moreover, Chatzigiannakou et al. provided a comprehensive discussion on the operational aspects of wave energy, including transportation logistics, deployment, costs, risk assessment of deployment, and maintenance of the Uppsala University Wave Energy Converter (UU WEC). [27]. Furthermore, recent advancements, such as CorPower's point absorber technology, have progressed beyond the demonstration phase and are moving towards commercial viability [28].

Wave energy technologies can be categorized into attenuators, point absorbers, and terminators based on device size and incoming wave direction [29]. Well-known examples of few technologies include Pelamis, CorPower's technology, and the UU WEC. For this work, we utilized Uppsala University's WEC which can be seen in Fig. 1. It is a point-absorber-based technology which is designed to operate in medium to deep waters [30]. Wave energy is directly converted into electricity using a linear generator, which produces voltage and current of varying frequency and amplitude due to ocean waves changing amplitude and frequency. Therefore, the fluctuating frequency and amplitude of the generated electrical power must be synthesized for safe grid integration or for isolated loads.

However, wave energy has yet to establish its niche in the commercial market due to its considerable size and higher

cost relative to the energy it generates [31], [32]. To make the wave energy industry profitable in the current utility grid market, WEC developers need to explore alternative pathways. One promising market is the off-grid sector, where wave energy can effectively supply power to regions where grid integration is challenging [33]. Examples include remote island electrification, water desalination systems [34], ocean surveillance systems [35], and recreational off-grid activities or resorts [36]. Additionally, energy storage solutions such as batteries can be used alongside WECs in a hybrid model to provide a constant power supply [37]. Hybrid energy systems, such as those that utilise a supercapacitor alongside a battery to manage higher frequency wave fluctuations, have shown a reduction in energy loss from the system while simultaneously enhancing battery life [38]. Energy storage has also been found to reduce the voltage and current harmonics at the wave energy system's Point of Common Coupling (PCC) [39]. For all these applications, the power generated by WECs must be synthesized, which can be achieved using power converters [40].

Recent advancements in power electronic converters and their control have made it possible to harvest wave energy and convert it into electrical power that can be directly connected to a three-phase load in an isolated mode forming a grid. A simple representation of a power flow from a WEC for island electrification can be seen in Fig. 2. Traditionally in a grid-connected system, WECs are connected to the grid, with the grid-side inverter controlled using a grid-following control [41]. In this approach, the grid ensures voltage stability, and the inverter follows the grid frequency using Phase-Locked Loop (PLL) control. In this setup, all the power generated by the WEC is transmitted to the grid [39].

Energy storage can be used to smooth out the variability in power produced by the WEC. When energy storage is included in the system, the control strategy changes. The inverter is then controlled to inject power according to the grid's demand for active and reactive power, while the energy storage controls the DC voltage. The surplus power is stored, and any power shortage is supplied from energy storage [37].

A bi-directional DC/DC converter connects energy storage to the DC bus. The energy storage control system is then implemented to control the switching of the DC/DC converter to maintain the DC bus voltage at a specified value. Different topologies of DC/DC converters can be used, and the selection criteria would depend on various factors such as the power level, input voltage range, required efficiency, control complexity, and cost. The final choice of topology is also influenced by the WEC design parameters, the rating of the wave energy farm, the wave climate, and the specific location of deployment. Groji et al. provide a comparative review of various DC-DC converter topologies, including their advantages and limitations [42]. Here, a boost converter is chosen as a DC / DC converter due to its simplicity in control, cost-effectiveness, and high efficiency for low to medium power levels.

FIGURE 2. Wave energy power flow.

For off-grid applications, the inverter is controlled to establish the required three-phase AC voltage and frequency, supplying the necessary current to the off-grid island load [43]. Deloading mode can be used to conserve energy at the DC bus and operate the system at 80-90% of its maximum capacity. This is typically achieved for wind turbines through pitch angle control. A similar strategy has not been reported for WECs. Therefore, incorporating energy storage with WECs can allow the system to have dispatchable energy features, which wave energy generally lacks.

Additionally, current and voltage harmonics pose significant challenges for wave energy converters at both grid integration points and in isolated grid operations [44]. These issues arise from the use of power electronic switches in direct-drive wave energy converter systems, combined with the intermittent nature of wave power. It is crucial to mitigate these harmonics at the PCC. Furthermore, the use of passive rectification for the generator converter can introduce additional current harmonics which can also lead to higher voltage harmonic issues at the PCC [39]. Hazra et al. propose the use of a SiC-based converter for wave energy systems and demonstrate its increased efficiency compared to a Si-based IGBT converter [45]. However, their study primarily focuses on comparing losses at different switching frequencies for standalone SiC and Si-based IGBT converters, with limited analysis of power quality in a unified wave energy system.

As more intermittent renewable energy sources are integrated into the grid through converter-based systems, reducing harmonics and fast transients at the PCC will likely become a priority for TSOs or in isolated load scenarios. Therefore, wave energy systems will need to adopt methods to further minimize harmonics to ensure safe connection to future electricity grids. Operating the grid/load-side converter at higher frequencies can help dampen fast oscillations within the system, thereby improving power quality. SiC-based converters enable switches to operate at these higher frequencies. This paper proposes and experimentally verifies the novel use of a SiC-based converter for wave energy systems to improve their power quality in a unified electrical system. This converter reduces load voltage and current harmonics in wave energy systems at the PCC.

A. PREVIOUS WORK ON WEC FOR OFF-GRID APPLICATIONS

Several studies have examined the integration of WEC into the electricity grid, but fewer have explored the potential of using wave energy for off-grid applications such as

electrifying remote islands. In [19], wave energy is proposed as a suitable power source for remote islands due to its substantial power potential. Various WEC technologies have been compared for different locations, with some technologies recommended based on factors such as power potential, water depth, and location. However, the electrical network and control aspects have not been covered in detail.

A case study on integrating wave energy for an Alaskan island is presented in [46]. This study includes a resource assessment compared with the time series of the island's community load, revealing that integrating wave energy can reduce diesel generator fuel consumption, leading to significant fuel cost savings. However, the electrical system for the island electrification, power management strategies and controls are lacking in this study.

Papers [47] and [48] simulate hybrid renewable power generation for island electrification. Paper [47] uses a hybrid wind-wave energy harvesting system for a remote island. Additionally, the proposed system in this paper also relies on diesel generators when renewable energy is not available. Paper [48] photovoltaic-wave energy hybrid renewable power generation systems for island electrification in Malaysia. The proposed system in this paper uses energy storage controlled by a DC/DC converter to balance power generation and load requirements. However, neither study considers power optimization control for the WEC. Additionally, these studies are simulation-based, and the implementation of the various controls for the island electrification is lacking. The examination of power quality issues concerning a wave energy system, particularly with respect to harmonics in voltage and current, is likewise not thoroughly addressed in these papers.

Papers [49] and [50] simulate WECs supplying power to isolated remote island loads, but both lack experimental validation of their control methods. Additionally, paper [49] does not address generator-side control for power optimization, and paper [50] involves energy storage at multiple locations in the electrical network, making the system relatively more expensive and increased computation due to energy storage system control.

Paper [51] focuses on power management in an islanded microgrid incorporating an AWS-based wave energy converter. Various operating scenarios were simulated based on the battery's state of charge (SOC). Paper [52] focuses on the mathematical modelling of the wave energy subsystem's hydrodynamic, mechanical, and electrical characteristics. It considers various operational modes, including islanded and grid-connected configurations. However, neither of these papers provides a detailed control loop design for the converters used in the electrical system. Furthermore, it is a simulation-based study and does not address harmonics components originating at the PCC from the WEC system.

B. CONTRIBUTIONS

As discussed above, several gaps exist in the experimental study of islanded electrification from a WEC system and its control. This paper addresses this gap by proposing and implementing a proof-of-concept of isolated Grid-Forming control (GFM) for the inverter to power an island load using a hybrid WEC and electrical energy storage system. The WEC is actively controlled using resistive loading complex conjugate control, while the battery storage system is controlled by a bi-directional DC/DC converter, charging and discharging based on WEC generation and load demand. The battery energy storage utilised in the system enhances the reliability and stability of the WEC system by managing the intermittent power generated. The comprehensive theory of different converter controls is experimentally verified using a physical back-to-back converter and a battery connected via a DC/DC converter. A controlled voltage source simulates a WEC, and a three-phase resistive load represents the island load.

Moreover, power quality issues continue to pose a significant challenge for various types of WEC system. Hence, a novel harmonics mitigation study for a WEC system was conducted by experimenting with the GFM control by using two different converter technologies. IGBT and SiC-based converters are tested individually for the load-side inverter at different switching frequencies, ranging from 5 kHz to 25 kHz. The maximum operating switching frequency for the SiC converter used in this study is 200 kHz, while for the Si-based IGBT converter, it is 30 kHz. Additionally, the Total Harmonic Distortion (THD) of the three-phase voltage current at the load is analyzed to ensure compliance with IEEE-recommended levels at the point of isolated load. This study directly compares the THD of load voltage and current between the SiC and IGBT converters at the same switching frequency condition.

Additional features are evaluated in conjunction with the experimental verification of the proposed control for various converters. Table. 1 compares the contribution of this paper and the existing research on WEC for remote islands electrification. It should be noted that for practical off-grid implementation, the inverter must be capable of transitioning seamlessly between isolated and grid-connected modes. Ullah et al. [20] presented a simulation-based study on multimode converter control, exploring transitions between various inverter modes, such as grid-following, grid-forming, and grid-supporting. This paper focuses on the experimental verification of an isolated grid forming control and harmonics mitigation using different converter technologies.
The primary contributions of this paper are as follows:

- Proposed the use of a wave energy converter to supply electricity to a remote island load in isolated mode.
- Implemented an isolated GFM control for the load-side inverter with a black start capability to supply power to an island load using a hybrid WEC.
- Designed and integrated an energy storage system control to enhance the reliability and stability of the WEC system.

TABLE 1. Comparison between the current paper and previous work on WEC for remote islands electrification.

Features	[19]	[46]	[47]	[48]	[49]	[50]	[51]	[52]	This paper
WEC as island's power system	✓	✓	✓	✓	✓	✓	✓	✓	✓
WEC side converter control		✓	✓			✓	✓	✓	✓
Load side grid-forming inverter control			✓	✓	✓	✓	✓		✓
Energy storage control				✓	✓	✓	✓		✓
Experimental study									✓
Isolated electrical system			✓	✓	✓	✓	✓		✓
Converter technology analysis (IGBT v/s SiC)									✓

- Designed the implemented control to minimize harmonics at the PCC, ensuring compliance with recommended standards.
- Experimentally verified the novel use of a SiC-based converter for wave energy applications to mitigate harmonics.
- Individually tested SiC-based and IGBT converters for harmonic performance at various switching frequencies using the proposed GFM control.

C. PAPER ORGANIZATION

The paper is organized as follows:

- Section II, the methodology section, explains the theory behind this experimental study and is divided into five subsections. First, the generation side, specifically the WEC and Permanent Magnet Linear Generator (PMLG), is explained. The subsequent subsections detail the control of the generator-side converter for optimal power absorption, the energy storage control to reduce WEC intermittency and manage the DC bus voltage control, and the GFM control for the load-side inverter. The last subsection compares the IGBT with the SiC-based converter and proposes the use of the SiC-based converter for wave energy converter applications.
- Section III goes through the different components used in the experimental study. This subsection also briefly discusses the practical challenges and limitations of the current experimental setup.
- Section IV presents and discusses the experimentally validated results of the proposed isolated GFM control in a WEC system. The load voltage and current harmonics results are shown to evaluate the power quality between IGBT and SiC-based converters separately.
- Section V concludes the work and summarizes the findings.

II. METHODOLOGY

This section defines the current system study's methodology and electrical network. The WEC used for the current study is discussed in subsection II-A. The generator-side converter control method is detailed in a subsequent subsection II-B. The battery energy storage control used to mitigate the WECs intermittency is explained in the subsection II-C. The load-side GFM control is derived in the subsection II-D. The final subsection II-E discusses the use of IGBT and SiC-based converters for WEC applications. Fig. 3 illustrates the complete electrical network of the system under study along with the generator side converter control.

A. WAVE ENERGY CONVERTER

Uppsala University designed a point absorber-based WEC which is used in this study. The entire system consists of a buoy tethered to a PMLG, which can be seen in Fig. 1. The buoy floats on the surface, whereas the generator is placed on the seabed. The power take-off (PTO) of this system is in a direct drive configuration, where the mechanical power from the wave is directly converted to electrical power without any intermediate power conversion. The direct drive PTO configuration is found to be the most feasible for slow-moving machines, such as the linear generator in a WEC [53]. However, this causes the output voltage and current to vary in both amplitude and frequency, which needs to be synthesized by power electronics converters to be safely connected to the electricity grid or a load [54]. This device is assumed to be restricted only to the heave motion. According to Newton's second law of motion, the force acting on the heaving PTO can be formulated as

$$m\ddot{\vec{z}}(t) = \vec{f_{ex}}(t) + \vec{f_r}(t) + \vec{f_b}(t) + \vec{f_l}(t) + \vec{f_{rs}}(t) + \vec{f_{pto}}(t) \quad (1)$$

where m is the total mass of the buoy, translator and the tether; $\ddot{\vec{z}}(t)$ is the heave acceleration of the buoy, tether and translator; $\vec{f_{ex}}(t)$ is the wave excitation force, $\vec{f_r}(t)$ is the wave radiation force, $f_b(t)$ is the buoyancy force, $f_l(t)$ is the losses, $\vec{f_{rs}}(t)$ is the restoring spring force; $\vec{f_{pto}}(t)$ is the control force applied by the PTO restoring force. The reader can refer to [55] and [56] for the detailed modelling of the different forces.

Further, the electrical system of a WEC consists of a PMLG and a generator-side converter to control the PTO force. This paper uses a direct-driven three-phase permanent magnet non-salient synchronous generator. Park transform then transforms the *abc* frame of reference to the *dq* frame of reference, which is used to model the linear generator. The *dq* component of the PMLG stator voltage can be expressed as

When velocity is positive:

$$\begin{cases} V_{d,g} = R_s i_{d,g} - \omega_e L_s i_{q,g} + L_s \dfrac{di_{d,g}}{dt} \\ V_{q,g} = R_s i_{q,g} - \omega_e L_s i_{d,q} + \omega_e \psi + L_s \dfrac{di_{q,g}}{dt} \end{cases} \quad (2)$$

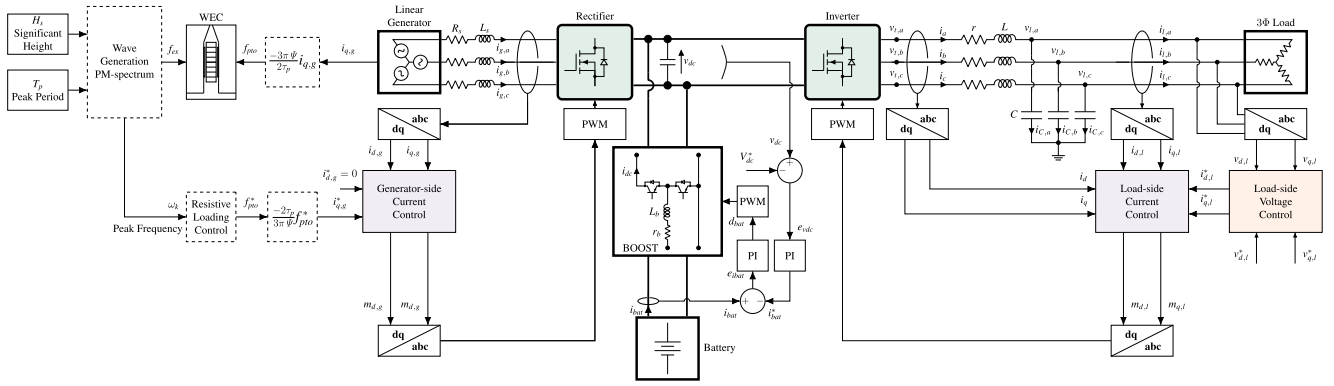

FIGURE 3. Schematic circuit of experimental setup.

When velocity is negative:

$$\begin{cases} V_{d,g} = R_s i_{d,g} + \omega_e L_s i_{q,g} - L_s \dfrac{di_{d,g}}{dt} \\ V_{q,g} = R_s i_{q,g} + \omega_e L_s i_{d,q} + \omega_e \psi - L_s \dfrac{di_{q,g}}{dt} \end{cases} \tag{3}$$

where i_g is the generator's stator current, R_s and L_s are the generator's synchronous resistance and inductance, ψ is stator winding flux linkage due to the permanent magnet and ω_e is the electrical angular frequency. It can be calculated by

$$\omega_e = \frac{\pi v}{\tau_p} \tag{4}$$

where v is the buoy and translator's velocity and τ_p is the pole pitch of the linear generator.

The input electromechanical power of the generator is given by

$$p_{pto} = \frac{3}{2}\frac{\pi}{\tau_p}\psi v i_{q,g} \tag{5}$$

The PTO power in terms of force and velocity can be written as

$$p_{pto} = -f_{pto} v \tag{6}$$

Substituting (5) in (6), gives

$$f_{pto} = -\frac{3\pi\psi}{2\tau_p} i_{q,g} \tag{7}$$

Hence, the PTO force can be directly controlled by controlling the linear generator's $i_{q,g}$ current. The remaining parameters are the design features of the generator, which can be seen in Table. 2.

B. GENERATOR SIDE CONVERTER CONTROL

The generator-side power converter can be used to control the damping of buoy motion to optimize power absorption from the WEC. The PMLG is controlled using the complex conjugate approach, which aims to maximize the energy captured by the WEC by making the translator velocity in phase with the excitation force with suitable amplitude [57].

TABLE 2. WEC parameters.

Parameter	Value
Buoy type	cylinder
Buoy radius (r)	2.5 m
Buoy draft (d)	1.5 m
Buoy and translator mass (m_b)	31000 kg
Water plane area (A_w)	19.6 m^2
Buoy infinite added mass (m_∞)	28518 kg
Buoyancy stiffness coefficient (S_b)	197370 N/m
Generator stroke z^*	2 m
End-stop spring coefficient (S_{es})	5 x 10^5 N/m
Restoring spring coefficient (S_{rs})	1 x 10^5 N/m
Generator peak flux (Φ put a cap)	0.1 Wb
Pole pitch (τ_p)	0.1 m
Number of turns of the stator coils (N)	300
Generator resistance (R_s)	0.2 Ω
Generator inductance (L_s)	32 mH
Sampling time (T_s)	2 x 10^{-4} s

This is achieved by cancelling out the intrinsic reactance and ensuring the PTO resistance equals the intrinsic resistance [58]. However, this control method requires knowledge of the buoy's future velocity, which determines the optimal generator force. To reduce complexity, a suboptimal control method is employed, utilizing the peak frequency of the wave spectrum instead, which makes the control causal [57].

There are two causal control methods: Approximate Complex-conjugate Control (ACC) and Resistive Loading Control (RLC). RLC is a passive damping control, while ACC is a reactive control, in which damping and stiffness are independently controlled [57]. ACC, a reactive control, allows bidirectional power flow between the PTO and the oscillating system, causing the PMLG to operate as a motor. In contrast, the RLC method provides a real damping force that is always positive, which means that the PMLG consistently functions as a generator. This method affects only the amplitude of the translator's velocity, not its phase [59].

This paper uses the RLC method to under-dimension the experimental setup deliberately. The peak-to-average power ratio can be in the range of $25.2 - 58.3$ in the case of ACC,

whereas the RLC method has a much lower peak-to-average power ratio, which can be in the range of 7.7 − 17.1 [60]. However, the generators and power electronics converters in the electrical system need to be designed for peak power. As the ACC method has a much higher peak power output, RLC was chosen to under-dimension the electrical circuit in the performed experiments. Additionally, the ACC method can only effectively transfer power for short wave periods centred around the peak natural frequency. With this method, generator losses increase significantly when the incident wave frequency deviates from the natural frequency. In contrast, the RLC method generates less power but is effective over a broader range of wave periods [57]. Therefore, the RLC method is chosen for WEC power optimization, with the paper focusing on the control and distribution of the generated WEC power for island electrification. The following equation represents the real and imaginary part of the PTO impedance for the optimal power absorption using the RLC method

$$\begin{aligned} r_{pto}^{op}(\omega_k) &= b(\omega_k) \\ x_{pto}^{op}(\omega_k) &= -\omega_k \left[m + m_{add}(\omega_k) + \frac{c}{\omega_k} \right] \end{aligned} \tag{8}$$

where ω_k is the peak frequency of the wave spectrum, $b(\omega_k)$ is the radiation damping coefficient at the peak frequency, m is the mass of the oscillating system, m_{add} is the added mass and c is the stiffness coefficient.

The reference PTO force is then calculated by

$$f_{pto}^{*}(\omega_k) = v\sqrt{\left(r_{pto}^{op}(\omega_k)\right)^2 + \left(x_{pto}^{op}(\omega_k)\right)^2} \tag{9}$$

where v is the velocity of the oscillating system. The reactive reference current $i_{q,g}$ can be then calculated using (7) and active reference current $i_{d,g}$ is kept at zero to reduce the copper losses [57]. The current control is then according to the block diagram shown in Fig. 5.

C. DC BUS VOLTAGE CONTROL

The battery system takes charge of regulating the DC-link bus voltage (v_{dc}). The DC bus voltage control is designed as a cascade control with two control loops. The primary loop (DC voltage) manages the main variable (v_{dc}) and the secondary loop (i_{bat}) addresses disturbances quickly, improving system precision and stability. By employing Kirchhoff's current law in the depicted Fig. 3, it gives rise to the differential equation

$$i_{bat} = i_{dc} + \frac{C_{eq} v_{dc}}{\mathrm{d}t}, \tag{10}$$

where i_{bat} is the battery current, v_{dc} voltage at the DC bus and i_{dc} is the input current of the inverter. The determination of the control gains for the outer voltage control loop is detailed in [49]

$$\begin{aligned} k_{p,vdc} &= 2\xi_{dc}\omega_{ndc}C_{eq} \\ k_{i,vdc} &= \omega_{ndc}^2 C_{eq}, \end{aligned} \tag{11}$$

where natural frequency, $\omega_{ndc} = 2\pi \times 128$ rad/s and damping ratio, $\xi_{dc} = 0.707$.

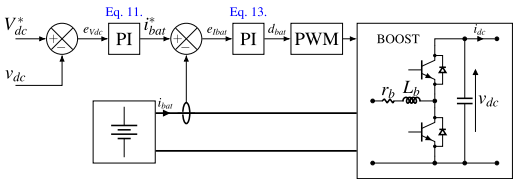

FIGURE 4. Block diagram of voltage and current control for the battery.

TABLE 3. Parameters of the battery controller.

Parameter	Value
Nominal voltage battery	100 V
Switching frequency	10 kHz
DC-Bus voltage	200 V
DC-Bus capacitor	C_{eq} = 3000 μF
L filter	r_b = 0.03 Ω and L_b = 4 mH
Current loop gains	$k_{p,ib}$ = 12.5 and $k_{i,ib}$ = 93.75
Battery rating	±6000W

The inner current control is modeled based on Kirchhoff's voltage law, and the following differential equation is obtained

$$L_b \frac{\mathrm{d}i_{bat}}{\mathrm{d}t} + r_b i_{bat} = v_{bat} - v_{t_{bat}}, \tag{12}$$

where $v_{t_{bat}}$ denotes the terminal voltage, v_{bat} represents the battery voltage of the battery converter, i_{bat} is the battery current, L_b is the inductor filter, and r_b is the internal resistance of the filter. Employing Pulse-width Modulation (PWM) as the converter's control strategy, it is acknowledged that $v_{t_{bat}} = d_b\, v_{dc}$.

The details regarding the calculation of control gains of the Proportional-integral (PI) controller for the outer voltage control loop are elaborated in [49].

$$\begin{aligned} k_{p,b} &= \frac{L_b}{\tau_{ib}} \\ k_{i,b} &= \frac{r_b}{\tau_{ib}}, \end{aligned} \tag{13}$$

where $\tau_{ib} = 0.32$ ms and $\tau_{ib} = 0.16$ ms. The block diagram representing the control of the battery system is depicted in Fig. 4.

Table. 3 outlines the key parameters of the battery system.

D. LOAD SIDE INVERTER CONTROL

In GFM mode, the load primarily dictates the inverter's behaviour. Unlike in grid-following mode, where the inverter synchronizes with the grid, in GFM mode, the inverter actively establishes the voltage and frequency reference. The inverter continuously adjusts its output to match the load's demand, ensuring stable voltage and frequency. Thus, the load's requirements directly influence the inverter's operations, making it the key factor in determining the system's overall behavior.

According to the model depicted in Fig. 3, Kirchhoff's voltage laws can be applied to write the AC voltage equations

for the three phases (a, b, c) of the inverter

$$L_{abc}\frac{\mathrm{d}i_{abc}}{\mathrm{d}t} = -r_{abc}i_{abc} + v_{t,abc} - v_{l,abc}, \tag{14}$$

where i_{abc} are the three-phase output currents (load current); $v_{t,abc}$ are the terminal voltages of the inverter; $v_{l,abc}$ are the AC voltages in the PCC. The impedance of the inverter is represented by a filter with inductance L_{abc} and internal resistance r_{abc}.

The output voltages $v_{l,abc}$, are obtained using Kirchhoff's current law

$$\frac{C\mathrm{d}v_{l,abc}}{\mathrm{d}t} = i_{c,abc} - i_{abc}. \tag{15}$$

The grid-forming mode is depicted within the synchronous reference frame (dq), where the modulation scheme employed is Sinusoidal Pulse-width Modulation (SPWM).

$$\begin{cases} L\dfrac{\mathrm{d}i_d}{\mathrm{d}t} = L\omega_s i_q + v_{d,t} - ri_d - v_{d,l} \\ L\dfrac{\mathrm{d}i_q}{\mathrm{d}t} = -L\omega_s i_d + v_{q,t} - ri_q - v_{q,l} \\ C\dfrac{\mathrm{d}v_{d,l}}{\mathrm{d}t} = C\omega_s v_{q,l} + i_d - i_{d,l} \\ C\dfrac{\mathrm{d}v_{q,l}}{\mathrm{d}t} = -C\omega_s v_{d,l} + i_q - i_{q,l}. \end{cases} \tag{16}$$

The *abc-dq* transformation introduces the d- and q-axis components of variables, represented by the subscripts d and q. Consequently, this transformation leads to cross-coupling phenomena in the equations, as exemplified by terms such as $\omega_s i_d$, $\omega_s i_q$, $\omega_s v_{l,d}$, and $\omega_s v_{l,q}$, where ω_s represents the angular frequency of the electrical system.

The electrical system's angular frequency—50 Hz in this study—is treated as a constant value rather than being actively controlled. By using a fixed angular frequency, the converter can generate the necessary voltage waveforms without the need for frequency tracking using phase-locked loop (PLL). Instead of implementing a PLL, grid-forming converters derive the phase angle by integrating the constant angular frequency over time. This approach allows the converter to maintain a stable reference for voltage and current waveform while simplifying the control requirements.

Following the transformation of three-phase voltage and current variables into dq signals through synchronous reference frame control [61], a cascade control strategy is implemented. This strategy employs two PI controllers, where the output of the AC voltage controller serves as the setpoint for the AC current controller, as depicted in Fig. 5.

The determination of the control gains for the inner current control loop is detailed in [49], [61]. It is recommended to select a value between 0.5 ms and 5 ms for τ_i, and in this study, we adopt 0.5 ms. The expressions for the PI control gains of the current control are given by:

$$\begin{aligned} k_{p,i} &= \frac{L}{\tau_i} \\ k_{i,i} &= \frac{r}{\tau_i}. \end{aligned} \tag{17}$$

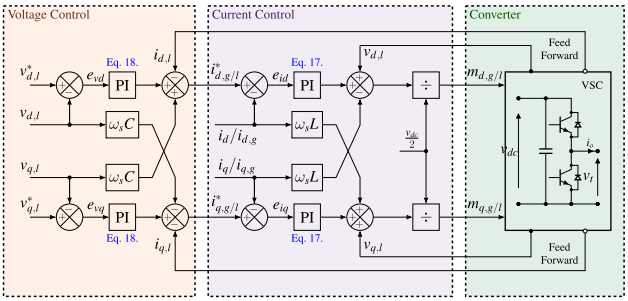

FIGURE 5. Block diagram of the grid forming inverter control.

TABLE 4. Parameters of the inverter.

Parameter	Value
Nominal load voltage (V_{rms})	105 V
Switching frequency	20 kHz
Nominal frequency	50 Hz
LC filter	$r = 0.3\ \Omega$, $L = 8$ mH and $C = 60\ \mu$F
3Φ load	$R_L = 65\ \Omega$
3Φ added load	$R_{added} = 105\ \Omega$
Current loop gains	$k_{p,i} = 16$ and $k_{i,i} = 600$
Voltage loop gains	$k_{p,v} = 0.0960$ and $k_{i,v} = 78.37$
Dead-time (IGBT)	1 μs
Dead-time (SiC)	0.1 μs

Drawing from the same references, the voltage control loop yields the following PI control gains:

$$\begin{aligned} k_{p,v} &= C\omega_n^2 \\ k_{i,v} &= 2C\xi\omega_n. \end{aligned} \tag{18}$$

Assuming a natural frequency of $\omega_n = 2\pi \times 182$ rad/s and a damping ratio of $\xi = 0.707$, the parameter values for the converter, as well as for the inner and outer loop control, are shown in Table. 4.

E. IGBT V/S SiC FOR WEC

In the past two decades, SiC has been recognized for its potential in high-temperature, high-power, high-frequency, and radiation-hardened applications due to its outstanding material properties: bandgap, thermal conductivity, melting temperature, and saturation drift velocity [62]. SiC has high power density and the capacity to process substantial power within a compact volume or area. This attribute is valuable in island electrification, where limited space and the need for robust, sustainable power solutions intersect. The superior thermal conductivity of SiC, combined with its high-temperature tolerance, facilitates efficient thermal management in compact designs. Therefore, SiC-based devices can reduce the need for bulky and expensive cooling systems while maintaining high reliability – resulting in considerable size and weight reductions for the WEC systems, which are crucial factors in their deployment and commercialization [63]. Besides, increasing the switching frequency would also decrease the component's size and weight, making it possible to place it on the WEC device even

though the cost of SiC-based devices still remains higher [64], [65]. In 2017, Wolfspeed, a Cree company, developed 900 V SiC MOSFET, which reduced EV drive-train losses by 78%, allowing a decrease in the battery pack size [66]. Moreover, the reliability test of commercially available SiC MOSFET with high humidity, 85%, and high temperature, 85 °C, showed stable performance of the device, which makes it suitable for wave energy applications [67]. SiC switch substitution resulted in a 50% reduction in energy loss per cycle, compared to common Si-based converters [68]. Conduction losses in SiC devices occur as current moves through the semiconductor components, primarily governed by the device's on-resistance. Unlike traditional silicon-based converters, SiC materials exhibit significantly lower on-resistance, translating to reduced power losses. This is critical in high-power applications where minimal heat generation per unit of current enables a smaller form factor without compromising durability. It was shown that conduction and switching losses are at least 3 times lower for SiC in DC-DC converters [69]. Also, a switching frequency above 20 kHz will reduce audible noise for humans, allowing the converter to be placed closer to the load [70].

Although SiC-based converters are more expensive than conventional converters, their high efficiency can offset the higher initial cost by minimizing losses [71]. Their enhanced reliability in offshore environments and improved efficiency offer significant advantages for wave energy applications where production components are located far from shore. This can potentially lower costs by reducing downtime and repair expenses. A study has demonstrated that the use of SiC increases power density and efficiency while also lowering life cycle costs and component costs [72]. In 2013, Nielsen et al. provided a comparison of Si IGBT and SiC FET, concluding that investment into a 2.5 times more expensive SiC converter can return within 772 days if the power supply is running at full power and 24 hours a day [73].

Despite the advantages of SiC-based converters and their fast-switching capabilities, several challenges remain. As a relatively new material, SiC has limited standardized converters available in the market. Additionally, higher switching frequencies in SiC-based converters can also increase parasitic capacitance, though research has focused on improved packaging to reduce parasitics and enhance heat dissipation for high-temperature operation. The increased switching frequency can further lead to challenges such as higher electromagnetic interference (EMI) levels, high dv/dt, and current oscillations [74]. Adding a small inductor at the SiC converter's output can help reduce current overshoot, parasitic capacitance, and dv/dt. Additionally, high-speed switching requires faster gate drivers to ensure the safe operation of the converter leg without the risk of short-circuiting. While SiC converters enable higher control bandwidth, there are still challenges in executing the control algorithm within each switching cycle, a concern that grows as the switching frequency increases [74].

III. EXPERIMENTAL SETUP

Experiments were conducted on a test bench setup to validate the controls involved in island electrification using a WEC. The experimental setup, shown in Fig. 6, includes Chroma's three-phase AC programmable voltage source, simulating the PMLG voltage source [75]. A linear generator model including WEC and the wave generation spectrum are developed in MATLAB/Simulink. The analog three-phase reference signals generated by the linear generator model in MATLAB/Simulink were then sent to the AC programmable device. The linear generator model then received current feedback from the external system as the reference current. This setup is also known as power hardware-in-the-loop, allowing us to simulate the linear generator model using the AC programmable device.

This voltage source is then connected to the machine-side converter via a machine inductor. The machine-side converter, a two-level (2-L) IGBT-based three-phase rectifier [76], is controlled to optimize power capture from the WEC as discussed in subsection II-B. In a 2-L converter, the voltage stress across the power switch equals the full DC bus voltage, resulting in large voltage steps and increased electromagnetic interference (EMI). Consequently, the real-world implementation of a 2-L converter requires careful filter design, additional shielding, and the inclusion of a common-mode filter.

Multilevel converters offer significant advantages over 2-L converters, including reduced EMI, lower common-mode voltage, and improved reliability [77]. Additionally, strategies such as optimizing the dead band, employing advanced carrier-based techniques (e.g., discontinuous DSVPWM or near-state methods), utilizing soft switching techniques, and incorporating snubber circuits can serve as effective alternatives to mitigate disturbances in 2-L converters. However, the current study is conducted under low voltage, low power, and balanced grid voltage conditions, where such disturbances have a minimal impact on the converter's efficiency. Hence, a 2-L converter was chosen for the current study.

Sensors are utilized to measure the voltage and current at different stages in real time, and the measured values are sent to the controller. Meanwhile, a central dSPACE controller performs calculations and generates PWM pulses for all converters (machine-side converter, DC/DC converter at the DC link, and load-side inverter).

It should be noted that this study utilizes a proof-of-concept for a single WEC system. A single WEC can be sufficient for smaller loads, such as surveillance systems, island communities with 20-30 houses, or resorts, which is the focus of this study. However, in reality the Uppsala University WEC concept envisions multiple WECs operating together to form a WEC farm system that supplies the island's load. Due to the constraints in creating a WEC farm using multiple controlled voltage source, this experimental study was conducted using only a single WEC. Additionally,

including multiple WECs would require an analysis of the wave energy park layout, which falls outside the scope of this paper. The challenges related to wave energy park optimization are addressed in Giassi et al. [78].

Chroma's bidirectional DC power supply simulates a battery [79]. It is then connected to the DC link via a half-bridge (Buck/Boost) converter [80]. A parallel capacitor is also connected to the DC bus to reduce voltage ripple. The rating of the battery would depend on the size of the WEC system and the island's load for a specific location, which is not covered in the current study.

The load-side inverter, a 2-L three-phase inverter, is connected to the DC link through an RLC filter [76]. Both IGBT-based and SiC-based switches were tested separately to assess power quality at the load. A Fluke's power quality and energy analyzer measured the THD of the three-phase load voltage and current [81]. The inverter's output is connected to three rheostat-based variable resistive loads in a star configuration, simulating an island load. Additional loads were connected in series with the existing load to test the controls under varying load conditions. Fig. 6 illustrates the experimental setup and the parameter values are provided in Table. 2, 3 and 4. In real-world implementations, including a star-delta transformer on the load side improves system stability, particularly during faults and unbalanced current conditions [82]. However, the current study focuses on a balanced load for experimental purposes, where the neutral current is consistently zero. Hence, the experiment is performed without the inclusion of a star-delta transformer.

It should also be noted that the type of load connected to the PCC is not a limiting factor in the grid-forming converters designed in this study. Instead, the load itself controls the system. The grid-forming converter is capable of detecting the load's requirements for active power, reactive power, or both, and it can adjust its output accordingly to meet these demands. However, due to the absence of a reactive load, only an active load was considered in this experimental study. A combined active and reactive load simulation study in a grid-forming mode can be found in Ullah et al. [49].

IV. RESULTS AND DISCUSSIONS

The experiments were conducted over a period of approximately $t = 150\,\text{s}$. The system operated under no-load conditions from $0\,\text{s} < t < 54\,\text{s}$. At $t = 54\,\text{s}$, the inverter was black-started, and the grid was formed for the R_L load. At $t = 100\,\text{s}$, an additional R_{added} load was connected to test the control under varying load conditions. The three-phase load voltage, current, and power quality were analyzed. Additionally, the load power quality was compared between IGBT and SiC-based inverters. The WEC generates power during the entire experimental period. The experiment was conducted at low power and voltage to protect the components because of the absence of protection circuits. Consequently, the required three-phase load rms voltage is set to 105 V. Optimization of the island's load, energy storage capacity, and WEC energy production for specific geographical locations is beyond the scope of this paper.

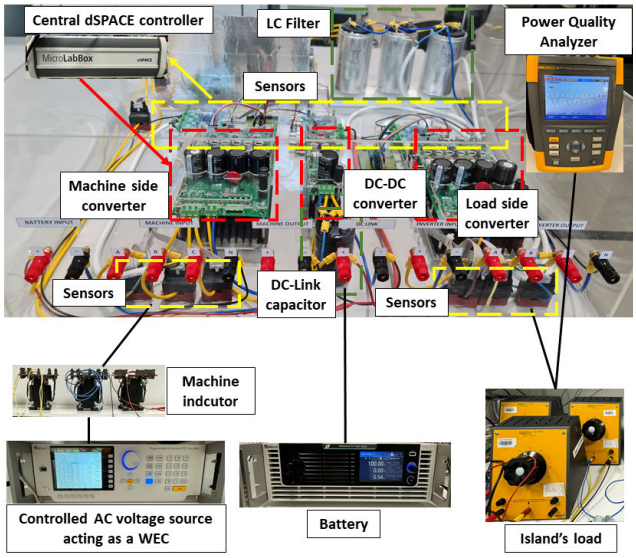

FIGURE 6. Experimental setup.

A. WEC GENERATOR-SIDE

The irregular wave profile is generated using a linear superposition of sinusoidal wave components derived from a predefined wave spectrum. Specifically, we employ the Pierson-Moskowitz (PM) spectrum, a widely used model for representing fully developed sea states. This spectrum defines the energy distribution of a wave as a function of angular frequency, based on significant wave height and time period [58], [83]. An irregular wave profile is used in this study, where the peak frequency of the wave spectrum, ω_k, is 1.2 rad/s.

The normalized emulated excitation force (maximum value of the excitation force), heave position, and velocity are shown in Fig. 7a. It can be seen from the magnified image in Fig. 7b. that the velocity and excitation forces are out of phase. This is due to the RLC method, which uses the total impedance of the intrinsic machine as the resistive loading or damping value to control the power, affecting only the amplitude and not the phase of the velocity [57]. Despite this, the RLC method is used in this study due to its ease of implementation, as discussed in the previous section. The varying amplitude and frequency of the three-phase current generated by the WEC are shown in Fig. 8.

The load-side inverter is initially turned off, resulting in zero three-phase load voltage and current. During this period from $0\,\text{s} < t < 54\,\text{s}$, the power generated by the WEC flows toward the energy storage system. The energy storage system control detects this and charges the battery accordingly, increasing the battery's SOC, as shown in Fig. 9b. The SOC decreases for the remaining time period. This is due to the addition of load. The energy storage controller effectively maintains the DC bus voltage at 200 V for the entire measurement period, as shown in Fig. 9a. For the

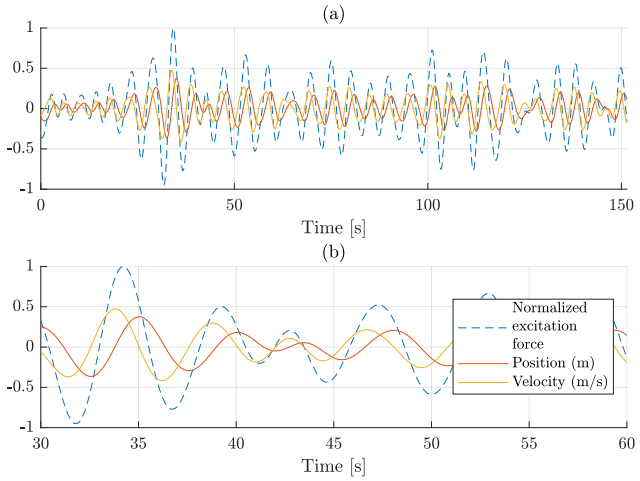

FIGURE 7. Normalized excitation force, position and velocity. (a) Full time frame (b) Magnified.

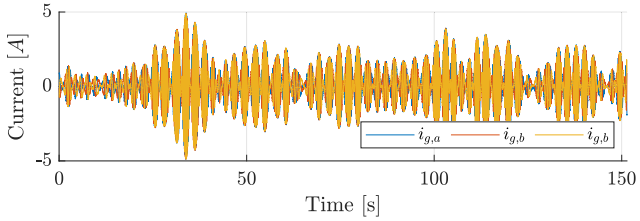

FIGURE 8. Linear generator current.

SOC to remain balanced and above zero for all scenarios, the energy demand of the remote island load must be balanced with the energy generated by the wave energy farm. This requires optimizing the size of the energy storage system, which depends on factors such as long-term wave forecasts, exact location, seasonal variations, and the size of the wave energy farm or converter, which is beyond the scope of this paper. The study related to the energy storage size for a wave energy converter can be found in Seyyedmahdi et al. [84].

B. LOAD-SIDE

The load-side inverter has a black start capability. At $t = 54$ s, the load-side inverter is turned on and the island load is supplied using the hybrid WEC and battery storage system. The GFM capability of the inverter generates a three-phase voltage at 50 Hz at the load bus and supplies the necessary three-phase AC current. The controller generates a three-phase AC voltage with a peak of 85 V at the load.

At $t = 100$ s, an additional resistive load, R_{added}, is connected. As shown in Fig. 10b and 10c, the d-axis current increases with the added load and effectively calculates and reaches its new reference, accompanied by increased power flow to the load. Despite this change, the d-axis voltage maintains the required load voltage, as illustrated in Fig. 10a. The three-phase current for the entire measurement period for the varying load condition is also shown in Fig. 11a. The magnified view of the three-phase AC load current for both loading conditions can be observed in Fig. 11b and 11c.

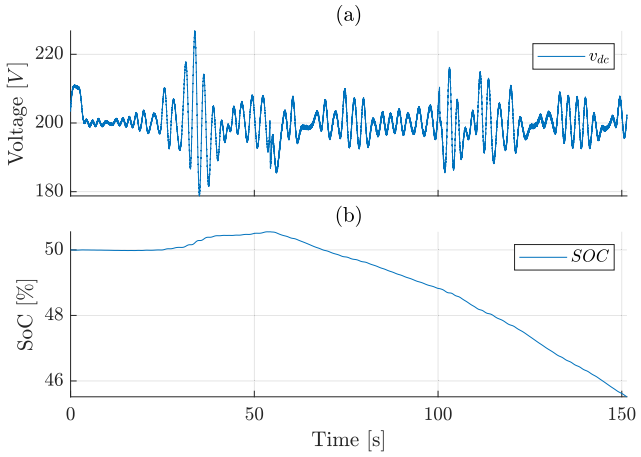

FIGURE 9. DC Bus. (a) DC link voltage (b) Battery's SOC.

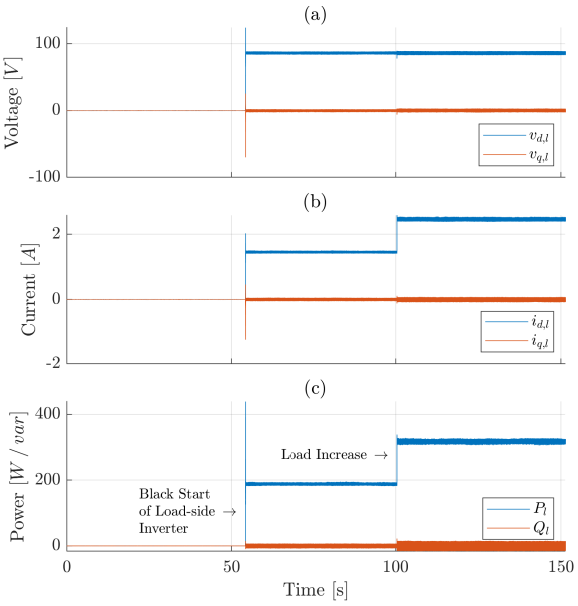

FIGURE 10. Load bus. (a) Voltage in *dq* frame. (b) Current in *dq* frame. (c) Load power.

Fig. 12 shows the oscilloscope measurements of the three-phase AC voltage and the single-phase AC current during two different load conditions and the load transition period. Fig. 12a and 12c demonstrate the steady-state response of the system. The controller successfully maintains a stable three-phase AC voltage at the required grid frequency of 50 Hz while supplying a stable current. Fig. 12b illustrates the dynamic response of the system. The controller's functionality is experimentally tested in load transition mode. It can be seen that, with a load change, the controller adjusts the AC load current quickly and smoothly. Meanwhile, the three-phase AC voltage remains stable, regardless of the change of load.

C. IGBT V/S SiC

The study was also conducted to compare the power quality at the load bus using IGBT or SiC-based converters. The

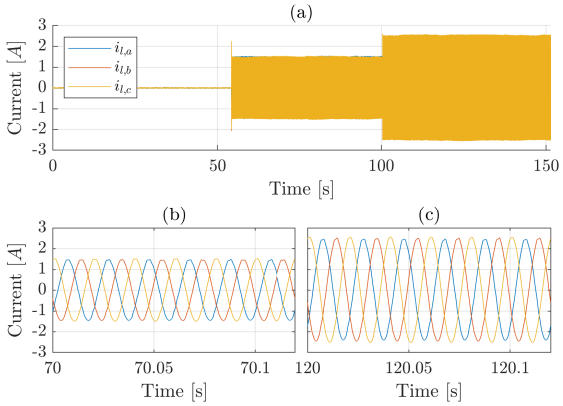

FIGURE 11. (a) Three-phase load current during the entire experimental time-frame. (b) Magnified steady state current with R_L load. (c) Magnified steady state current after the addition of R_{added} load.

THD of the load's three-phase AC voltage and current was examined for switching frequencies ranging from 5 kHz to 25 kHz, in 5 kHz increments. Both IGBT or SiC-based inverters were tested individually. According to IEEE Standard 519, the voltage distortion limit, or THD, at the PCC for voltages less than 1kV should be below 8.0% [85]. However, harmonics need to be more carefully regulated for isolated loads [86]. Therefore, this paper chooses a stricter voltage THD limit of 5.0%. Similarly, the current distortion, according to IEEE Std 1547, should be below 5.0% [87].

As shown in Fig. 13, the THD of both the load voltage and current remains below the IEEE recommended limit of 5% for all switching frequencies. At the lowest switching frequency of 5 kHz, the voltage and current THD for both IGBT and SiC-based converters are comparable, with SiC having a lower THD. However, as the switching frequency increases, the voltage and current THD of the IGBT inverter increase, reaching a maximum current THD of 4% at 25 kHz. In contrast, the SiC-based converter exhibits significantly lower current THD, with a value of 0.9% at 25 kHz. In summary, the THD voltage at the load of the SiC-based converter is approximately 92% lower than that of the IGBT at 25 kHz. Furthermore, the current THD at the load from the SiC-based converter is about 78% lower than that of the IGBT at the same switching frequency. This suggests that SiC-based technology typically offers enhanced power quality at all switching frequencies and the added benefit of a lower component weight and size at higher frequencies, as outlined in subsection I-B. Therefore, using a SiC-based converter at higher switching frequencies can significantly benefit WEC systems by improving power quality and reducing the weight of electrical components, making WEC systems more suitable for cheaper and easier deployment.

To investigate the frequencies that contribute to the THD, the voltage and current harmonics for both IGBT and SiC-based converter can be seen in Fig. 14. In the case of IGBT, the harmonic content of three-phase load voltage and current is majorly the 5th (250 Hz) and 7th (350 Hz)

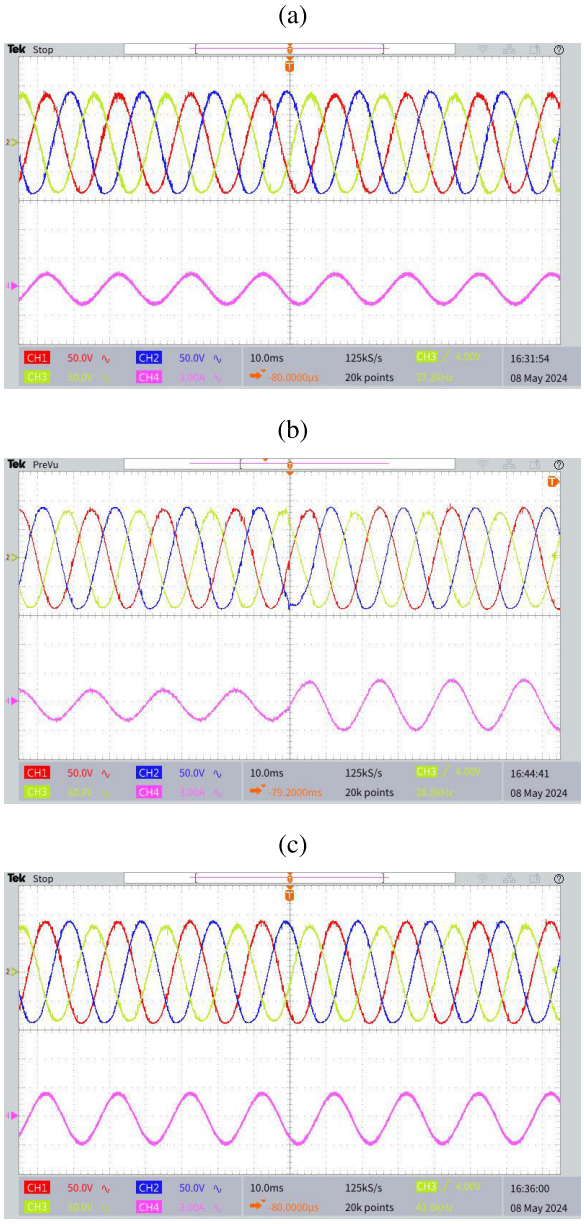

FIGURE 12. Three-phase load voltage and one-phase load current. (a) R_L load. (b) Load transition period. (c) Addition of R_{added} load.

harmonic, which can be seen in Fig. 14a and 14c. This is due to the pulse width modulation technique used in the inverter, which introduces the lowest-order harmonics. The harmonic being situated closer to the fundamental frequency of 50 Hz can make it challenging to filter. However, in the case of SiC, the lower 5th and 7th harmonics are negligible due to much lower dead time, turn on and turn off time compared to the IGBT and do not need to be filtered. This can be seen in Fig. 14b and 14d.

V. CONCLUSION

This paper presents an electrical approach to remote island electrification using a WEC. Generator-side, load-side converter and battery energy storage control methodologies are

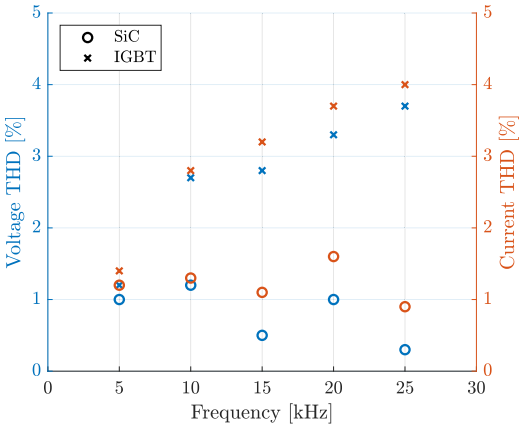

FIGURE 13. Load voltage(in blue) and current(in red) THD at different inverter switching frequencies for both SiC and IGBT converters.

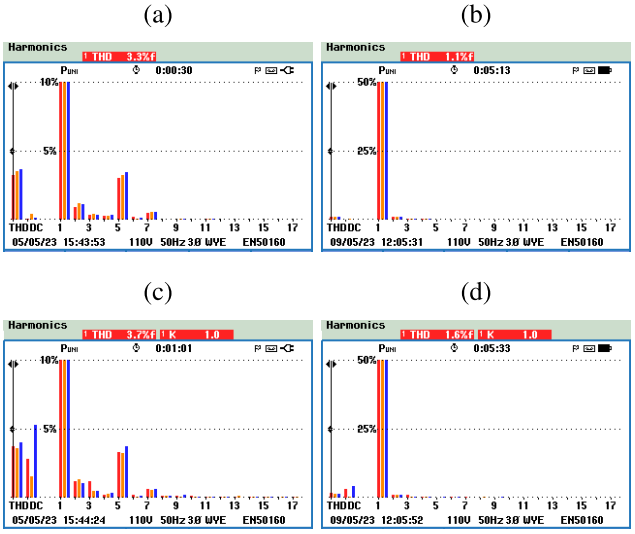

FIGURE 14. THD component measured from 'Fluke 430 Power Qualityand Energy Analyzers at 20 kHz switching frequency. (a) Load voltage (IGBT). (b) Load voltage (SiC). (c) Load current (IGBT). (d) Load current (SiC).

proposed and experimentally tested. The RLC method is utilized to optimize power absorption by the WEC, providing a damping force that affects the amplitude of the WEC's velocity, thereby enhancing its power output. Energy storage is implemented and controlled to mitigate the variability of WEC power. The DC-link voltage is shown to be effectively maintained at approximately 200 V. To maintain a constant DC-link voltage in all weather scenarios, the size of the energy storage must be balanced with the dimensions of the island load, the wave energy converter, and its energy output. Consequently, additional research is necessary to tailor the system for particular locations, wave forecasts, and seasonal conditions variations.

GFM control establishes the island's three-phase AC voltage of 85 V peak and frequency at 50 Hz, delivering a stable AC current to the three-phase resistive loads. The controller also maintains a constant load voltage and increases the AC load current in a few milliseconds when the load increases. The load-side converter also provides black start functionality. The power quality from the proposed isolated GFM control, in terms of AC voltage and current THD, is experimentally measured and found to be below the limit of 5%. Furthermore, the paper compares IGBT and SiC converters, revealing that SiC converters produce better voltage and current THD at all the switched frequencies tested. At 5 kHz, the power quality of both IGBT and SiC converters is comparable. As the switching frequency rises from 5 kHz to 25 kHz in 5 kHz increments, the THD of voltage and current from the IGBT also rises. However, in the SiC converter, the voltage and current harmonic components are further reduced. At a switching frequency of 25 kHz, the SiC converter significantly improves power quality by reducing the voltage THD from 3.7% to 0.3% and the current THD from 4% to 0.9%. Overall, the use of SiC-based converter reduces the voltage THD by 92% and current THD by 78% at 25 kHz of switching frequency. Moreover, the SiC converter produces minimal low-frequency fifth- and seventh-harmonic components in voltage and current when compared to the IGBT, significantly diminishing the necessity for extra filtering circuits. Therefore, using SiC converters can enhance power quality and reduce the weight and size of components, providing a significant advantage for WEC systems.

Although the present work lacks research on the environmental issues arising from the installation of wave energy converter machines, it highlights that environmental concerns such as effects on local flora and fauna need further study prior to installing such a WEC system. Additionally, engaging in dialogue and reaching a local consensus for such systems is essential. Previous research has shown promising results for niche markets such as island electrification. This paper provides the technical aspects, including system design, controls and harmonics mitigation for a WEC-based grid-isolated system. The dynamic stability of the control system during the transition from a grid-connected system to a grid-isolated system is planned for future work.

REFERENCES

[1] S. K. Singal, Varun, and R. P. Singh, "Rural electrification of a remote island by renewable energy sources," *Renew. Energy*, vol. 32, no. 15, pp. 2491–2501, Dec. 2007.
[2] K. Matsumoto and Y. Matsumura, "Challenges and economic effects of introducing renewable energy in a remote island: A case study of Tsushima Island, Japan," *Renew. Sustain. Energy Rev.*, vol. 162, Jul. 2022, Art. no. 112456.
[3] G. Asplund, "Application of HVDC light to power system enhancement," in *Proc. IEEE Power Eng. Soc. Winter Meeting. Conf.*, vol. 4, Jul. 2000, pp. 2498–2503.
[4] L. Tripathi, A. K. Mishra, A. K. Dubey, C. B. Tripathi, and P. Baredar, "Renewable energy: An overview on its contribution in current energy scenario of India," *Renew. Sustain. Energy Rev.*, vol. 60, pp. 226–233, Jul. 2016.
[5] G. Singh, P. Baredar, A. Singh, and D. Kurup, "Optimal sizing and location of PV, wind and battery storage for electrification to an Island: A case study of Kavaratti, Lakshadweep," *J. Energy Storage*, vol. 12, pp. 78–86, Aug. 2017.
[6] A. H. Fathima and K. Palanisamy, "Optimization in microgrids with hybrid energy systems—A review," *Renew. Sustain. Energy Rev.*, vol. 45, pp. 431–446, May 2015.

[7] V. Khare, S. Nema, and P. Baredar, "Status of solar wind renewable energy in India," *Renew. Sustain. Energy Rev.*, vol. 27, pp. 1–10, Nov. 2013.

[8] V. Khare, S. Nema, and P. Baredar, "Solar–wind hybrid renewable energy system: A review," *Renew. Sustain. Energy Rev.*, vol. 58, pp. 23–33, Jan. 2016.

[9] A. Singh, P. Baredar, and B. Gupta, "Computational simulation & optimization of a solar, fuel cell and biomass hybrid energy system using Homer pro software," *Proc. Eng.*, vol. 127, pp. 743–750, May 2015.

[10] G. L. Kyriakopoulos and G. Arabatzis, "Electrical energy storage systems in electricity generation: Energy policies, innovative technologies, and regulatory regimes," *Renew. Sustain. Energy Rev.*, vol. 56, pp. 1044–1067, Apr. 2016.

[11] G. Bekele and G. Tadesse, "Feasibility study of small hydro/PV/wind hybrid system for off-grid rural electrification in Ethiopia," *Appl. Energy*, vol. 97, pp. 5–15, Sep. 2012.

[12] A. Blavette, "Grid integration of wave energy & generic modelling of ocean devices for power system studies," Ph.D. thesis, Hydraul. & Maritime Res. Centre (HMRC), Nat. Univ. Ireland, Univ. College Cork, Ireland, 2013.

[13] Y. Kuang, Y. Zhang, B. Zhou, C. Li, Y. Cao, L. Li, and L. Zeng, "A review of renewable energy utilization in islands," *Renew. Sustain. Energy Rev.*, vol. 59, pp. 504–513, Jun. 2016.

[14] T. Weir, "Renewable energy in the Pacific Islands: Its role and status," *Renew. Sustain. Energy Rev.*, vol. 94, pp. 762–771, Oct. 2018.

[15] T. Ahmad and D. Zhang, "Renewable energy integration/techno-economic feasibility analysis, cost/benefit impact on islanded and grid-connected operations: A case study," *Renew. Energy*, vol. 180, pp. 83–108, Dec. 2021.

[16] P. Bertheau, "Supplying not electrified islands with 100% renewable energy based micro grids: A geospatial and techno-economic analysis for the Philippines," *Energy*, vol. 202, Jul. 2020, Art. no. 117670.

[17] L. F. Prieto, G. R. Rodríguez, and J. S. Rodríguez, "Wave energy to power a desalination plant in the north of gran Canaria Island: Wave resource, socioeconomic and environmental assessment," *J. Environ. Manage.*, vol. 231, pp. 546–551, Feb. 2019.

[18] B. Robertson, J. Bekker, and B. Buckham, "Renewable integration for remote communities: Comparative allowable cost analyses for hydro, solar and wave energy," *Appl. Energy*, vol. 264, Apr. 2020, Art. no. 114677.

[19] M. Fadaeenejad, R. Shamsipour, S. D. Rokni, and C. Gomes, "New approaches in harnessing wave energy: With special attention to small Islands," *Renew. Sustain. Energy Rev.*, vol. 29, pp. 345–354, Jan. 2014.

[20] M. I. Ullah, J. S. Döhler, V. M. de Albuquerque, J. Forslund, C. Boström, and I. Temiz, "Multi-mode converter control for linear generator-based wave energy system," *IET Renew. Power Gener.*, vol. 18, no. 8, pp. 1520–1534, Jun. 2024.

[21] M. G. Hughes and A. D. Heap, "National-scale wave energy resource assessment for Australia," *Renew. Energy*, vol. 35, no. 8, pp. 1783–1791, Aug. 2010.

[22] A. Angelis-Dimakis, M. Biberacher, J. Dominguez, G. Fiorese, S. Gadocha, E. Gnansounou, G. Guariso, A. Kartalidis, L. Panichelli, I. Pinedo, and M. Robba, "Methods and tools to evaluate the availability of renewable energy sources," *Renew. Sustain. Energy Rev.*, vol. 15, no. 2, pp. 1182–1200, Feb. 2011.

[23] B. Drew, A. Plummer, and M. N. Şahinkaya, "A review of wave energy converter technology," *Proc. Inst. Mech. Eng. A, J. Power Energy*, vol. 223, no. 8, pp. 887–902, Jul. 2009.

[24] J. P. Sierra, C. Mösso, and D. González-Marco, "Wave energy resource assessment in Menorca (Spain)," *Renew. Energy*, vol. 71, pp. 51–60, Nov. 2014.

[25] G. Iglesias and R. Carballo, "Wave resource in el Hierro—An island towards energy self-sufficiency," *Renew. Energy*, vol. 36, no. 2, pp. 689–698, Feb. 2011.

[26] J. E. Stopa, K. F. Cheung, and Y.-L. Chen, "Assessment of wave energy resources in Hawaii," *Renew. Energy*, vol. 36, no. 2, pp. 554–567, Feb. 2011.

[27] M. A. Chatzigiannakou, "Offshore deployments of marine energy converters," Ph.D. dissertation, Dept. Elect. Eng., Uppsala Univ., Acta Universitatis Upsaliensis, Uppsala, Sweden, 2019.

[28] B. Joensen and H. B. Bingham, "Economic feasibility study for wave energy conversion device deployment in faroese waters," *Energy*, vol. 295, May 2024, Art. no. 130869.

[29] I. López, J. Andreu, S. Ceballos, I. M. de Alegría, and I. Kortabarria, "Review of wave energy technologies and the necessary power-equipment," *Renew. Sustain. Energy Rev.*, vol. 27, pp. 413–434, Nov. 2013.

[30] A. Parwal, F. Remouit, Y. Hong, F. Francisco, V. Castelucci, L. Hai, L. Ulvgård, W. Li, E. Lejerskog, and A. Baudoin, "Wave energy research at Uppsala University and the Lysekil research site, Sweden: A status update," in *Proc. 11th Eur. Wave Tidal Energy Conf.*, Nantes, France, Sep. 2015, pp. 1–12.

[31] D. Clemente, P. Rosa-Santos, and F. Taveira-Pinto, "On the potential synergies and applications of wave energy converters: A review," *Renew. Sustain. Energy Rev.*, vol. 135, Jan. 2021, Art. no. 110162.

[32] E. Meneses, R. Soria, J. Portilla, W. Guachamín-Acero, R. Álvarez, R. Paredes, and M. Arias-Hidalgo, "The potential of wave energy converters in the Galapagos Islands," *Energy Strategy Rev.*, vol. 54, Jul. 2024, Art. no. 101457.

[33] H. Nilsson, "Off-grid market opportunities for wave power technology," Division Prod. Manage., Lund Univ., Lund, Sweden, Tech. Rep., 2016. [Online]. Available: https://lup.lub.lu.se/luur/download?func=downloadFile&recordOId=8892284&fileOId=8892285

[34] E. Ramudu, "Ocean wave energy-driven desalination systems for off-grid coastal communities in developing countries," in *Proc. IEEE Global Humanitarian Technol. Conf.*, Oct. 2011, pp. 287–289.

[35] I. McLeod and J. V. Ringwood, "Powering data buoys using wave energy: A review of possibilities," *J. Ocean Eng. Mar. Energy*, vol. 8, no. 3, pp. 417–432, Aug. 2022.

[36] A. Sandberg, E. Klementsen, G. Müller, A. De Andres, and J. Maillet, "Critical factors influencing viability of wave energy converters in off-grid luxury resorts and small utilities," *Sustainability*, vol. 8, no. 12, p. 1274, Dec. 2016.

[37] M. I. Ullah, J. S. Döhler, D. C. Silva Júnior, C. Boström, J. G. Oliveira, and I. Temiz, "Analysis of a hybrid energy storage system in a grid-tied wave energy converter for varying power demand," in *Proc. 11th Int. Conf. Renew. Power Gener.-Meeting Net Zero Carbon (RPG)*, Sep. 2022, pp. 218–222.

[38] X. Zhu, X. Huang, and X. Xiao, "Fast nonlinear model predictive control for the energy management of hybrid energy storage system in wave energy converters," *IEEE Trans. Ind. Electron.*, early access, Jan. 30, 2025, doi: 10.1109/TIE.2025.3531458.

[39] M. I. Ullah, I. Temiz, J. Forslund, and J. S. Döhler, "Power quality assessment of a wave energy converter using energy storage," in *Proc. Eur. Wave Tidal Energy Conf.*, vol. 15, Sep. 2023, Paper 315-1.

[40] J. Burhanudin, A. S. A. Hasim, A. M. Ishak, J. Burhanudin, and S. M. F. B. S. M. Dardin, "A review of power electronics for nearshore wave energy converter applications," *IEEE Access*, vol. 10, pp. 16670–16680, 2022.

[41] H. A. Said and J. V. Ringwood, "Grid integration aspects of wave energy—Overview and perspectives," *IET Renew. Power Gener.*, vol. 15, no. 14, pp. 3045–3064, Oct. 2021.

[42] S. A. Gorji, H. G. Sahebi, M. Ektesabi, and A. B. Rad, "Topologies and control schemes of bidirectional DC–DC power converters: An overview," *IEEE Access*, vol. 7, pp. 117997–118019, 2019.

[43] J. S. Döhler, R. P. Mota, J. A. G. Archetti, D. C. S. Júnior, C. Boström, and J. G. Oliveira, "An application of four-wire grid-forming power inverter in unbalanced distribution network," *IET Gener., Transmiss. Distribution*, vol. 17, no. 2, pp. 324–336, Jan. 2023.

[44] M. Penalba and J. Ringwood, "A review of wave-to-wire models for wave energy converters," *Energies*, vol. 9, no. 7, p. 506, Jun. 2016.

[45] S. Hazra, "Power generation and energy storage integration for wave energy conversion system," Doctoral dissertation, Dept. Eng. Res. Center, Future Renewable Elect. Energy Del. Manage. (FREEDM) Syst. Center, North Carolina State Univ., Raleigh, NC, USA, 2017.

[46] S. J. Beatty, P. Wild, and B. J. Buckham, "Integration of a wave energy converter into the electricity supply of a remote Alaskan Island," *Renew. Energy*, vol. 35, no. 6, pp. 1203–1213, Jun. 2010.

[47] S. Rasool, K. M. Muttaqi, and D. Sutanto, "A novel configuration of a hybrid wind-wave energy harvesting system for a remote island," in *Proc. IEEE Ind. Appl. Soc. Annu. Meeting (IAS)*, Oct. 2021, pp. 1–6.

[48] N. H. Samrat, N. B. Ahmad, I. A. Choudhury, and Z. B. Taha, "Modeling, control, and simulation of battery storage photovoltaic-wave energy hybrid renewable power generation systems for island electrification in Malaysia," *Sci. World J.*, vol. 2014, pp. 1–21, May 2014.

[49] M. I. Ullah, J. S. Döhler, V. Albuquerque, C. Boström, and I. Temiz, "Grid-forming control for the linear-generator-based wave energy converter for the electrification of remote islands," in *Proc. 12th Int. Conf. Power Electron., Mach. Drives (PEMD)*, vol. 2023, Oct. 2023, pp. 264–270.

[50] M. C. Sousounis, L. K. Gan, A. E. Kiprakis, and J. K. H. Shek, "Direct drive wave energy array with offshore energy storage supplying off-grid residential load," *IET Renew. Power Gener.*, vol. 11, no. 9, pp. 1081–1088, Jul. 2017.
[51] Q. Chuan, M. Jin, S. Chen, and X. Wang, "Decentralized power management of an islanded microgrid with AWS-based wave energy converter," in *Proc. 12th IEEE PES Asia–Pacific Power Energy Eng. Conf. (APPEEC)*, Sep. 2020, pp. 1–5.
[52] P. B. Garcia-Rosa, J. P. V. S. Cunha, F. Lizarralde, S. F. Estefen, I. R. Machado, and E. H. Watanabe, "Wave-to-wire model and energy storage analysis of an ocean wave energy hyperbaric converter," *IEEE J. Ocean. Eng.*, vol. 39, no. 2, pp. 386–397, Apr. 2014.
[53] N. J. Baker, "Linear generators for direct drive marine renewable energy converters," Ph.D. dissertation, Dept. Elect. Eng., Durham Univ., Durham, U.K., 2003.
[54] C. Boström, "Electrical systems for wave energy conversion," Ph.D. dissertation, Dept. Elect. Eng., Uppsala Univ., Acta Universitatis Upsaliensis, Uppsala, Sweden, 2011.
[55] A. Wahyudie, O. Saeed, M. Jama, H. Noura, and K. Harib, "Maximising power conversion for heaving point absorbers using a reference-based control technique," *IET Renew. Power Gener.*, vol. 11, no. 3, pp. 271–280, Feb. 2017.
[56] A. Y. Elamin, A. Wahyudie, T. B. Hashfi, H. Shareef, R. Errouissi, M. S. Laghari, M. B. Mubin, and S. Mekhilef, "Real-time model predictive control framework for a point absorber wave energy converter with excitation force estimation and prediction," *IEEE Access*, vol. 12, pp. 4078–4098, 2024.
[57] A. de la Villa Jaén, A. García-Santana, and D. E. Montoya-Andrade, "Maximizing output power of linear generators for wave energy conversion," *Int. Trans. Electr. Energy Syst.*, vol. 24, no. 6, pp. 875–890, Jun. 2014.
[58] J. Falnes and A. Kurniawan, *Ocean Waves and Oscillating Systems: Linear Interactions Including Wave-Energy Extraction*, vol. 8. Cambridge, U.K.: Cambridge Univ. Press, 2020.
[59] M. C. Sousounis and J. Shek, "Wave-to-wire power maximization control for all-electric wave energy converters with non-ideal power take-off," *Energies*, vol. 12, no. 15, p. 2948, Jul. 2019.
[60] E. Tedeschi, M. Carraro, M. Molinas, and P. Mattavelli, "Effect of control strategies and power take-off efficiency on the power capture from sea waves," *IEEE Trans. Energy Convers.*, vol. 26, no. 4, pp. 1088–1098, Dec. 2011.
[61] A. Yazdani and R. Iravani, *Voltage-Sourced Converters in Power Systems: Modeling, Control, and Applications*, 1st ed., Hoboken, NJ, USA: Wiley, 2010.
[62] X. She, A. Q. Huang, Ó. Lucía, and B. Ozpineci, "Review of silicon carbide power devices and their applications," *IEEE Trans. Ind. Electron.*, vol. 64, no. 10, pp. 8193–8205, Oct. 2017.
[63] Y. Bérubé, A. Ghazanfari, H. F. Blanchette, C. Perreault, and K. Zaghib, "Recent advances in wide bandgap devices for automotive industry," in *Proc. 46th Annu. Conf. IEEE Ind. Electron. Soc.*, Oct. 2020, pp. 2557–2564.
[64] J. Loncarski, H. A. Hussain, and A. Bellini, "Efficiency, cost, and volume comparison of SiC-based and IGBT-based full-scale converter in PMSG wind turbine," *Electronics*, vol. 12, no. 2, p. 385, Jan. 2023.
[65] C. Fjellstedt, M. I. Ullah, J. Forslund, E. Jonasson, I. Temiz, and K. Thomas, "A review of AC and DC collection grids for offshore renewable energy with a qualitative evaluation for marine energy resources," *Energies*, vol. 15, no. 16, p. 5816, Aug. 2022.
[66] Wolfspeed. (2024). *Wolfspeed Introduces New SiC MOSFET for EV Drive Trains*. Accessed: Jun. 11, 2024.[Online]. Available: https://www.wolfspeed.com/company/news-events/news/wolfspeed-introduces-new-sic-MOSFET-for-ev-drive-trains/
[67] J. B. Casady, B. Hull, J. Zhang, D. Gajewski, G. Wang, S. Allen, J. Palmour, and K. Olejniczak, "First automotive reliability assessment and drive-train performance of large-area 900V, 10mOhm SiC MOSFETs," in *Proc. IEEE Appl. Power Electron. Conf. Expo. (APEC)*, Mar. 2017, pp. 2259–2262.
[68] T. Todorcevic, P. Bauer, and J. A. Ferreira, "Efficiency improvements using SiC MOSFETs in a DC–DC modular multilevel converter for renewable energy extraction," in *Proc. 16th Int. Power Electron. Motion Control Conf. Expo.*, Sep. 2014, pp. 514–520.
[69] M. Alam, K. Kumar, and V. Dutta, "Comparative efficiency analysis for silicon, silicon carbide MOSFETs and IGBT device for DC–DC boost converter," *Social Netw. Appl. Sci.*, vol. 1, no. 12, pp. 1–11, Dec. 2019.
[70] D. W. Hart and D. W. Hart, *Power Electronics*, vol. 166. New York, NY, USA: McGraw-Hill, 2011.
[71] J. Biela, M. Schweizer, S. Waffler, and J. W. Kolar, "SiC versus Si—Evaluation of potentials for performance improvement of inverter and DC–DC converter systems by SiC power semiconductors," *IEEE Trans. Ind. Electron.*, vol. 58, no. 7, pp. 2872–2882, Jul. 2011.
[72] R. M. Burkart and J. W. Kolar, "Comparative life cycle cost analysis of Si and SiC PV converter systems based on advanced η-ρ-σ multiobjective optimization techniques," *IEEE Trans. Power Electron.*, vol. 32, no. 6, pp. 4344–4358, Jun. 2017.
[73] R. Ø. Nielsen, L. Török, S. Munk-Nielsen, and F. Blaabjerg, "Efficiency and cost comparison of Si IGBT and SiC JFET isolated DC/DC converters," in *Proc. 39th Annu. Conf. IEEE Ind. Electron. Soc.*, Nov. 2013, pp. 695–699.
[74] X. Yuan, I. Laird, and S. Walder, "Opportunities, challenges, and potential solutions in the application of fast-switching SiC power devices and converters," *IEEE Trans. Power Electron.*, vol. 36, no. 4, pp. 3925–3945, Apr. 2021.
[75] Chroma. (2023). *61509 Programmable AC Power Data Sheet*. Accessed: May 27, 2024. [Online]. Available: https://www.chromausa.com/pdf/61509%20Programmable%20AC%20Power%20052023.pdf
[76] Taraz Technol. (2024). *SPM-VFD Data Sheet*. Accessed: May 27, 2024. [Online]. Available: https://www.tarazteчnologies.com/Downloads/Datasheets/SPM-VFD.pdf
[77] N. S. Hasan, N. Rosmin, D. A. A. Osman, and A. H. Musta'amal@Jamal, "Reviews on multilevel converter and modulation techniques," *Renew. Sustain. Energy Rev.*, vol. 80, pp. 163–174, Dec. 2017.
[78] M. Giassi, "Numerical and experimental modelling for wave energy arrays optimization," Ph.D. dissertation, Dept. Elect. Eng., Uppsala Univ., Acta Universitatis Upsaliensis, Uppsala, Sweden, 2020.
[79] Chroma. (2024). *62000D Bidirectional DC Power Supply Data Sheet*. Accessed: May 27, 2024. [Online]. Available: https://www.chromausa.com/pdf/62000D%20Bidirectional%20DC%20Power%20Supply%20052024.pdf
[80] Taraz Technol. (2024). *SPM-HB Data Sheet*. Accessed: May 27, 2024. [Online]. Available: https://www.tarazteчnologies.com/Downloads/Datasheets/SPM-HB.pdf
[81] Fluke Corp. *Fluke 430 Series Li Power Quality and Energy Analyzers Data Sheet*. Accessed: May 27, 2024. [Online]. Available: https://dam-assets.fluke.com/s3fs-public/Fluke-430-II-PQ-Analysers-Data-Sheet.PDF?jvpPx9LB3aVXQ4WeJmcUc5FXfjXq.ULW
[82] D. B. Kanase and H. T. Jadhav, "Three-phase distribution static compensator for power quality improvement," *J. Inst. Engineers India, B*, vol. 103, no. 5, pp. 1809–1826, Oct. 2022.
[83] A. Pecher and J. P. Kofoed, *Handbook of Ocean Wave Energy*. Cham, Switzerland: Springer, 2017.
[84] S. Jafarishiadeh and M. Farasat, "Modeling and sizing of an undersea energy storage system," *IEEE Trans. Ind. Appl.*, vol. 54, no. 3, pp. 2727–2739, May 2018.
[85] *IEEE Standard for Harmonic Control in Electric Power Systems*, IEEE Standard 519-2022, 2022, pp. 1–31.
[86] *IEEE Guide for Design, Operation, and Integration of Distributed Resource Island Systems With Electric Power Systems*, IEEE Standard 1547.4-2011, 2011, pp. 1–54.
[87] *IEEE Standard for Interconnection and Interoperability of Distributed Energy Resources With Associated Electric Power Systems Interfaces*, IEEE Standard 1547-2018, 2018, pp. 1–138.

MD IMRAN ULLAH (Graduate Student Member, IEEE) received the B.Tech. degree in electrical and electronics engineering from Manipal Institute of Technology, Karnataka, India, in 2017, and the M.Sc. degree in renewable electricity production from Uppsala University, Sweden, in 2020, where he is currently pursuing the Ph.D. degree in electrical engineering. He was a Visiting Researcher with United Arab Emirates University (UAEU), United Arab Emirates, in 2024. His research interests include the grid integration of renewable energy, particularly wave energy, as well as power electronics control strategies, AC/DC/AC converters, energy management systems, and power quality.

TUANKU BADZLIN HASHFI (Graduate Student Member, IEEE) received the B.Eng. degree (Hons.) in electrical and electronics engineering from the National University of Malaysia, Selangor, Malaysia, in 2015, and the M.Eng.Sc. degree from the University of Malaya, Malaysia, in 2021. He is currently pursuing the Ph.D. degree with TU Delft, The Netherlands. Then, he was with United Emirates Arab University (UAEU), as a Research Assistant, until June 2024. His research interests include dc/dc converters, ac/dc converters, multilevel converters, modular multilevel converters (MMC), the control strategies, renewable energy conversion, and high voltage direct current (HVdc).

JESSICA S. DÖHLER received the M.Sc. degree in electronic systems in 2020. She is currently pursuing the Ph.D. degree in electrical engineering with Uppsala University. She is also actively involved in projects focused on advanced control strategies for microgrids, contributing to innovations in decentralized energy management, and grid stability. Her research interests include static converters for grid interfacing and the integration of renewable energy sources into electrical power systems.

VINICIUS M. DE ALBUQUERQUE received the B.S. and M.Sc. degrees in electrical engineering from the Federal University of Juiz de Fora (UFJF), Juiz de Fora, Brazil, in 2017 and 2020, respectively. He is currently pursuing the Ph.D. degree with a special focus on generator design for efficient energy harvesting with Uppsala University, Uppsala, Sweden. During both degrees, he acted as Undergraduate (from 2013 to 2017) and Graduate (from 2018 to 2019) Researcher with the Modern Lighting Research Group (NIMO), Engineering School, UFJF. He was a beneficiary of Brazilian Program Science Without Borders, completing two semesters with the University of Minnesota, Minneapolis, MN, USA, from 2015 to 2016. His current research interests include electronic energy conversion, hydropower, hydro-oscillating power conversion, and the modeling and control of electronic power converters for grid connection and permanent magnet synchronous machines.

AISULUU AITKULOVA received the master's degree in applied mathematics and physics from the Skolkovo Institute of Science and Technology, in 2020. She is currently pursuing the Ph.D. degree with the Department of Electrical Engineering, Uppsala University. She is also developing an integration process for 2D materials and wide-bandgap semiconductors for electronics, with a focus on graphene and diamond.

JOHAN FORSLUND received the master's degree in engineering physics in 2012 and the Ph.D. degree in electrical systems for marine current power in 2018. He is currently an Assistant Professor of power electronics for synchronous machines with the Department of Electrical Engineering, Uppsala University. He is also involved on grid connection and control of ocean energy-based systems for energy conversion.

CECILIA BOSTRÖM received the M.Sc. degree in engineering science and the Ph.D. degree in engineering science with specialization in science of electricity from Uppsala University, Uppsala, Sweden, in 2006 and 2011, respectively. She is currently an Associate Professor and the Head of the Department of Electrical Engineering, Uppsala University. Her research interest includes electrical systems for various applications.

ADDY WAHYUDIE received the B.Eng. degree in electrical engineering from Gadjah Mada University, Indonesia, in 2002, the M.Eng. degree in electrical engineering from Chulalongkorn University, Thailand, in 2005, and the D.Eng. degree in electrical engineering from Kyushu University, Japan, in 2010. From 2005 to 2011, he was a Lecturer with the Department of Electrical Engineering, Gadjah Mada University. In 2011, he joined United Arab Emirates (UAE) University, as an Assistant Professor. He is currently an Associate Professor with the Department of Electrical Engineering, UAE University. His research interests include control systems applications in electromechanical and renewable energy systems (ocean wave).

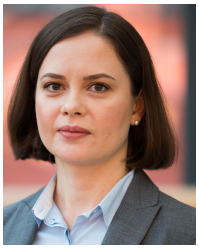

IRINA TEMIZ received the Ph.D. degree in mathematics from Novosibirsk State University, Russia, in 2008. She became a Docent of engineering physics with Uppsala University, Sweden, in 2019. She has been a Senior Lecturer with Uppsala University and has researched within the offshore energy field, since 2012. From 2016 to 2017, she was also involved in research and development at Swedish wave energy company Seabased. She has researched within fields of offshore renewable energy, particularly wave energy, control, grid integration, and power quality.